

Optical spectroscopic observations of γ -ray blazar candidates IV

Results of the 2014 follow-up campaign

F. Ricci^{1,2}, F. Massaro^{3,4}, M. Landoni⁵, R. D'Abrusco², D. Milisavljevic²,
D. Stern⁶, N. Masetti⁷, A. Paggi², Howard A. Smith², G. Tosti⁸
riccif@fis.uniroma3.it

Received October 15, 2014; accepted ...

Abstract

The extragalactic γ -ray sky is dominated by the emission arising from blazars, one of the most peculiar classes of radio-loud active galaxies. Since the launch of *Fermi* several methods were developed to search for blazars as potential counterparts of unidentified γ -ray sources (UGSs). To confirm the nature of the selected candidates, optical spectroscopic observations are necessary. In 2013 we started a spectroscopic campaign to investigate γ -ray blazar candidates selected according to different procedures. The main goals of our campaign are: 1) to confirm the nature of these candidates, and 2) whenever possible determine their redshifts. Optical spectroscopic observations will also permit us to verify the robustness of the proposed associations and check for the presence of possible source class contaminants to our counterpart selection. This paper reports the results of observations carried out in 2014 in the Northern hemisphere with Kitt Peak National Observatory (KPNO) and in the Southern hemisphere with the Southern Astrophysical Research (SOAR) telescopes. We also report three sources observed with the Magellan and Palomar telescopes. Our selection of blazar-like sources that could be potential counterparts of UGSs is based on their peculiar IR colors and on their combination with radio observations both at high and low frequencies (i.e., above and below ~ 1 GHz) in publicly available large radio surveys. We present the optical spectra of 27 objects. We confirm the blazar-like nature of 9 sources that appear to be potential low-energy counterparts of UGSs. Then we present new spectroscopic observations of 10 active galaxies of uncertain type associated with *Fermi* sources, classifying all of them as blazars. In addition, we present the spectra for five known γ -ray blazars with uncertain redshift estimates and three BL Lac candidates that were observed during our campaign. We also report the case for *WISE* J173052.85-035247.2, candidate counterpart of the source 2FGL J1730.6-0353, which has no radio counterpart in the major radio surveys. We confirm that our selection of γ -ray blazars candidates can successfully identify low-energy counterparts to *Fermi* unassociated sources and allow us to discover new blazars.

Subject headings: galaxies: active - galaxies: BL Lacertae objects - radiation mechanisms: non-thermal

1. Introduction

Blazars are the largest population of active galactic nuclei (AGNs) detected in the γ range (Abdo et al. 2010; Nolan et al. 2012). Their non-thermal emission ex-

¹Dipartimento di Matematica e Fisica, Università Roma Tre, via della Vasca Navale 84, I-00146, Roma, Italy

²Harvard - Smithsonian Center for Astrophysics, 60 Garden Street, Cambridge, MA 02138, USA

³Dipartimento di Fisica, Università degli Studi di Torino, via Pietro Giuria 1, I-10125 Torino, Italy

⁴Yale Center for Astronomy and Astrophysics, Physics Department, Yale University, PO Box 208120, New Haven, CT 06520-8120, USA

⁵INAF-Osservatorio Astronomico di Brera, Via Emilio Bianchi 46, I-23807 Merate, Italy

⁶Jet Propulsion Laboratory, California Institute of Technology,

4800 Oak Grove Drive, Mail Stop 169-221, Pasadena, CA 91109, USA

⁷INAF - Istituto di Astrofisica Spaziale e Fisica Cosmica di Bologna, via Gobetti 101, 40129, Bologna, Italy

⁸Dipartimento di Fisica, Università degli Studi di Perugia, 06123 Perugia, Italy

tends from radio to TeV energies and it is coupled with very rapid variability, high and variable polarization, superluminal motion, high luminosities (e.g., Urry & Padovani 1995) and peculiar infrared (IR) colors (Massaro et al. 2011a). Since 1978, well before the establishment of the unification scenario for the AGNs, their peculiar properties were described in terms of emission arising from particles accelerated in a relativistic jet closely pointed along our line of sight (Blandford & Rees 1978).

Adopting the nomenclature of the blazar subclasses described in the Roma-BZCAT: Multi-frequency Catalogue of Blazars¹ (e.g., Massaro et al. 2009; Massaro et al. 2011b), we distinguish between BL Lac objects (i.e., BZBs) and the flat spectrum radio quasars indicated as BZQs. The former present optical spectra with emission and/or absorption lines of rest frame equivalent width $EW \leq 5 \text{ \AA}$ (e.g., Stickel et al. 1991; Stoke et al. 1991; Laurent-Muehleisen et al. 1999) while the latter show typical quasar-like optical spectra with strong and broad emission lines. In the Roma-BZCAT there are also several BZBs indicated as BL Lac candidates; these sources were indicated as BL Lacs in literature and thus reported in the catalog but, lacking their optical spectra, a correct classification is still uncertain (see also Massaro et al. 2014a).

We developed several methods to search for γ -ray blazar candidates that could be counterparts of the unidentified γ -ray sources (UGSs, 2FGL Nolan et al. 2012) on the basis of the peculiar IR colors of known γ -ray blazars (e.g. D’Abrusco et al. 2013; Massaro et al. 2013a; Massaro et al. 2013b), discovered thanks to all-sky survey of the Wide-Field Infrared Survey Explorer (WISE; Wright et al. 2010), or using radio observations in combination with IR colors (Massaro et al. 2012c) as well as at low frequencies in the MHz regime (Massaro et al. 2012b; Nori et al. 2014). In addition, multifrequency analysis based on X-ray follow-up observations (e.g., Mirabal & Halpern 2009; Paggi et al. 2013; Takeuchi et al. 2013; Stroh et al. 2013; Acero et al. 2013) and radio campaigns (e.g., Petrov et al. 2013) were performed to search for potential UGS counterparts.

Since the positional uncertainty of *Fermi* is a few tenths of a degree, all the proposed methods and the multifrequency follow-up observations are primarily useful to decrease the number of potential counterparts for the UGSs. There could be possible contamination by different source classes in

these selection procedures of γ -ray blazar candidates (e.g., Stern & Assef 2013) and such degeneracy can be only removed with optical spectroscopic observations (e.g., Masetti et al. 2013; Shaw et al. 2013a; Shaw et al. 2013b; Paggi et al. 2014; Massaro et al. 2014a). Furthermore, a detailed knowledge of the number of UGSs is of paramount importance for instance to provide constraints on dark matter models (Abdo et al. 2014). Many UGSs could be blazars, but how many of them are actually blazars is still unknown due in part to the incompleteness of catalogs used for the associations (Ackermann et al. 2011a).

Thus, motivated by these arguments, we started an optical spectroscopic campaign in 2013 aiming to confirm the real nature of the proposed low-energy counterparts of UGSs selected according to our methods.

In this paper we report the results of observations carried out since January 2014 in both hemispheres. We mainly used the Kitt Peak National Observatory (KPNO) for our targets in the Northern hemisphere in addition to two more observations performed at Palomar. For targets mainly visible in the Southern sky, we present spectra obtained with the Southern Astrophysical Research (SOAR) telescope and one more observation carried out at Magellan. Preliminary results for our exploratory program in the Northern hemisphere obtained with the Telescopio Nazionale Galileo (TNG), the Multiple Mirror Telescope (MMT) and the Observatorio Astronómico Nacional (OAN) in San Pedro Mártir (México) were already presented in Paggi et al. (2014). In addition, the results of our observations carried out in the 2013 campaign with SOAR and KPNO are described by Landoni et al. (2014) and Massaro et al. (2014b), respectively.

The paper is organised as follows: Section 2 contains the different methods that we employed for the sample selection, in Section 3 we present our observational setup and we discuss the data reduction procedures. Then in Section 4 we describe the results of our analysis for different types of sources in our sample. Finally, Section 5 is devoted to summary and conclusions. We use cgs units unless otherwise stated.

2. Selecting the sample

The surveys and the catalogs used to search for the counterparts of our targets are listed in the following. These symbols are also reported in Table 1. Below 1GHz we used the VLA Low-Frequency Sky Survey Discrete Source Catalog (VLSS; Cohen et al. 2007, -

¹ <http://www.asdc.asi.it/bzcat/>

V) and the recent revision VLLSr² (Lane et al. 2014), the Westerbork Northern Sky Survey (WENSS; Rengelink et al. 2007, - W), the Sydney University Molonglo Sky Survey (SUMSS; Mauch et al. 2003, - S), the Parkes-MIT-NRAO Surveys (PMN; Wright et al. 1994, - Pm), the Parkes Southern Radio Source catalog (PKS; Wright et al. 1990, - Pk), and the Low-frequency Radio Catalog of Flat-spectrum Sources (LORCAT; Massaro et al. 2014b, - L). At higher radio frequencies we also verified the counterparts in the NRAO VLA Sky Survey³ (NVSS; Condon et al. 1998, - N), the Australia Telescope 20 GHz Survey (AT20G; Murphy et al. 2010, - A), the Combined Radio All-Sky Targeted Eight-GHz Survey (CRATES; Healey et al. 2007, - c). In the infrared, we queried the *WISE* all-sky survey in the AllWISE Source catalog⁴ (Wright et al. 2010, - w) and the Two Micron All Sky Survey (2MASS; Skrutskie et al. 2006, - M) since each *WISE* source is automatically matched to the closest 2MASS potential counterpart (see Cutri et al. 2012, for details). Then, we also searched for optical counterparts, with or without possible spectra available, in the Sloan Digital Sky Survey Data Release 9 (SDSS DR9; e.g. Ahn et al. 2012, - s), in the Six-degree-Field Galaxy Redshift Survey (6dFGS; Jones et al. 2004; Jones et al. 2009, - 6). At high-energies, in the X-rays, we searched the ROSAT all-sky survey in both the ROSAT Bright Source Catalog (RBSC; Voges et al. 1999, - X) and the ROSAT Faint Source Catalog (RFSC; Voges et al. 2000, - X), as well as *XMM-Newton* Slew Survey (XMMSL; Saxton et al. 2008; Warwick et al. 2012, - x), the Deep *Swift* X-Ray Telescope Point Source Catalog (1XSPS; Evans et al. 2014, - x), the *Chandra* Source Catalog (CSC; Evans et al. 2010, - x) and the *Swift* X-ray survey for all *Fermi* UGSs (Stroh et al. 2013). Note that we use the same symbol for the X-ray catalogs of *XMM-Newton*, *Chandra* and *Swift*.

Our sample lists a total of 27 sources divided as follows: 9 are UGSs for which the analysis based on the IR colors of blazar candidates indicated them as blazar-like sources that were observed during our campaign; 10 are indeed classified as active galaxies of uncertain type (AGUs) according to The Second Catalog of Active Galactic Nuclei Detected by the Fermi Large

Area Telescope (2LAC; Ackermann et al. 2011a) for which no optical spectra were available when the catalog was released and have been observed as part of our campaign. Some sources have been also selected based on low-frequency radio information (Massaro et al. 2013b). The remaining 8 sources are BL Lac candidates and BL Lacs, either detected or not by *Fermi* listed in the Roma-BZCAT for which no optical spectroscopic information were found in literature (Massaro et al. 2011b) or with uncertain/unknown redshift estimate.

We discuss our spectroscopic analysis in the following subsections while in Table 1 we summarize our results and report the multifrequency notes for each source with the only exceptions of those listed in the Roma-BZCAT. The finding charts for all the sources are shown in Figures 1-3 using the USNO-B1 Catalog (Monet et al. 2003) and the Digitized Sky Survey⁵. We highlight that some of the sources observed during our campaign have also been observed at different observatories and groups. However we re-observed these targets for two main reasons: 1) when our observations were scheduled and performed these spectra were not yet published; 2) due to the well-known BL Lac variability in the optical energy range, there is always the chance to observe the source during a quiescent or low state and detect some emission and/or absorption features that could allow us to constrain their redshifts.

3. Observations and Data Reduction

Optical spectra of most of the sources accessible from the Northern hemisphere were acquired in remote observing mode with the KPNO Mayall 4-m telescope using the R-C spectrograph, while the sources in the Southern hemisphere were observed remotely with the SOAR 4-m telescope using the High Throughput Goodman spectrograph. We also present the optical spectrum of the source *WISE* J024440.30-581954.5, observed on UT 2014 February 3 in visitor mode at Las Campanas Observatory using the Magellan 6.5-m telescope in combination with the IMACS instrument. Finally, we present optical spectra of *WISE* J025333.64+321720.8 and *WISE* J085654.85+714623.8 obtained in visitor mode on UT 2014 February 22 with the Double Spectrograph (DBSP) at the Hale 200-inch Telescope at Palomar Observatory. Our scientific goal, i.e. the classification of

²<http://heasarc.gsfc.nasa.gov/W3Browse/all/vlssr.html>

³<http://heasarc.gsfc.nasa.gov/W3Browse/radio-catalog/nvss.html>

⁴<http://wise2.ipac.caltech.edu/docs/release/allwise/>

⁵<http://archive.eso.org/dss/dss>

the selected targets, is best achieved with broad spectral coverage. We thus adopted a slit width of $1.2''$ ($1''$) and the low resolution gratings yielding a dispersion of ~ 3 (2) \AA pixel^{-1} for KPNO (SOAR). Our observations took place the nights UT 2014 June 4 and 5 at KPNO and on UT 2014 April 24 at SOAR during grey time. The average seeing for both runs was about $1''$ and conditions were clear. Additional observations were made on 2014 February 3 with the 6.5m Baade Magellan telescope using the Inamori Magellan Areal Camera and Spectrograph (IMACS; Bigelow et al. 1998). The $f/2$ camera was used in combination with the 300 mm^{-1} grism (blaze angle 17.5 degrees) and a $0.7''$ slit to yield spectra with dispersion of $1.34 \text{\AA pixel}^{-1}$ and FWHM resolution of $\sim 4 \text{\AA}$. Conditions were photometric and the seeing was generally $< 1''$. The whole set of spectroscopic data acquired at these telescopes was optimally extracted (Horne 1986) and reduced following standard procedures with IRAF (Tody 1986). For each acquisition we performed bias subtraction, flat field correction and cosmic rays rejection. Since for each target we secured two individual frames, we averaged them according to their signal to noise ratios (SNR). For questionable spectral features, we have exploited the availability of two individual exposures in order to better reject spurious signals. The wavelength calibration was achieved using the spectra of He-Ne-Ar or Hg-Ar lamps that assure coverage of the entire range. To take into account drift and flexures of the instruments during the night, we took an arc frame before each target to guarantee a good wavelength solution for the scientific spectra. The achieved accuracy is about ~ 0.3 (0.4) \AA rms for KPNO (SOAR). Although our program did not require accurate photometric precision, we observed a spectrophotometric standard star to perform relative flux calibration on each spectrum. Finally, we corrected the whole sample for the Galactic absorption assuming E_{B-V} values computed using the Schlegel et al. (1998) and Cardelli et al. (1989) relations. To better detect faint spectral features and measure redshifts, we normalised each spectrum to its continuum. For the Palomar observations, we observed the candidates through a $1.5''$ slit with the $\sim 5500 \text{\AA}$ dichroic to split the light across the blue and red arms of DBSP. Both sides have had resolving powers $R \equiv \lambda/\Delta\lambda \sim 1000$, and the data were reduced as above.

4. Results

4.1. Unidentified Gamma-ray Sources

Here we provide details for the low-energy counterparts of the 9 UGSs observed in our sample. All these *WISE*-selected counterparts were found in the analysis performed by Massaro et al. (2013a) to have IR *WISE* colors similar to known γ -ray blazars. All of them were predicted to be BZB-like sources having the IR colors more consistent with those of the *Fermi* BZBs rather than the BZQs (see D'Abrusco et al. 2013, for more details). The spectra of the whole UGSs listed in Table 1 are shown in Figure 4-12. The blazar counterpart for one of these sources, *WISE* J173052.85-035247.2 (candidate counterpart of 2FGL J1730.6-0353) appears intriguing. On the basis of our optical spectra, we classify the source as a BL Lac object and we put a lower limit on its redshift of 0.776 based on the detection of an intervening doublet system of Mg II ($\lambda\lambda_{obs} = 4965 - 4977 \text{\AA}$ with $EW_{obs} = 3.4 - 2.1 \text{\AA}$; see also Figure 9). However, this source is not associated with any NVSS sources, as expected for BL Lac objects. We note that, even if deeper radio observations detect emission from the source, blazars are traditionally defined as radio-loud sources on the basis of current radio data. All confirmed blazar in Roma-BZCAT are indeed detected at 1.4 GHz with fluxes above a few mJy, and radio-quiet blazars are extremely rare objects (Londish et al. 2004; Paggi et al. 2013). In particular, only 14 BZBs out of the 1220 present in the Roma-BZCAT have a radio flux density at 1.4GHz lower than 2.5 mJy that is the average flux limit of the NVSS survey⁶.

There are two sources, *WISE* J174507.82+015442.4 and *WISE* J174526.95+020532.6, potential counterparts to 2FGL J1745.6+0203 found on the basis of the IR color selection method. According to our multifrequency investigation we note that only *WISE* J174507.82+015442.4 has a radio counterpart, thus we conclude that *WISE* J174526.95+020532.6 is a normal radio-quiet quasar contaminating our selection. However we cannot firmly establish the real blazar nature of *WISE* J174507.82+015442.4 since the lack of multi-wavelength radio observations did not allow us to verify the flatness of its radio spectrum. For both objects we determined their redshifts based on broad emission lines ($H\alpha$ and $H\beta$ are both present, see Figures 10-11).

⁶<http://heasarc.gsfc.nasa.gov/W3Browse/radio-catalog/nvss.html>

Table 1: Selected sample and observation log. The sample is divided into three subsamples that are: potential counterparts of the UGSs, sources classified as AGUs, BL Lac candidates and BL Lacs with uncertain redshift listed in the Roma-BZCAT. Among the Roma-BZCAT sources, those marked with an asterisk are detected by *Fermi* (Nolan et al. 2012). Symbols used for the multifrequency notes are described in Sec. 2.

Name	<i>Fermi</i> name	R.A. (J2000)	Dec. (J2000)	Obs. Date (yyyy-mm-dd)	Exp. (s)	notes	class	z
J112325.37-252857.0	2FGL J1123.3-2527	11:23:25.37	-25:28:57.0	2014-04-23	300	N,w,M,6,U,g - ($z=0.145784$ -QSO-Jones+09)	QSO	0.148
J125949.80-374858.1	2FGL J1259.8-3749	12:59:49.80	-37:48:58.2	2014-04-23	600	S,N,w,U	BL Lac	?
J132840.61-472749.2	2FGL J1328.5-4728	13:28:40.43	-47:27:48.7	2014-04-23	600	S,rf,w,M,U,g,u,x - SED in Takeuchi+13	BL Lac	?
J134042.01-041006.8	2FGL J1340.5-0412	13:40:42.01	-04:10:07.2	2014-06-05	1200	N,F,w,U,u,x - SED in Takeuchi+13	BL Lac	?
J134706.88-295842.4	2FGL J1347.0-2956	13:47:06.88	-29:58:42.5	2014-04-23	900	S,N,rf,w,M,U	BL Lac	?
J173052.85-035247.2	2FGL J1730.6-0353	17:30:52.86	-03:52:47.2	2014-06-05	900	w,M	BL Lac	≥ 0.776
J174507.82+015442.4	2FGL J1745.6+0203	17:45:07.82	+01:54:42.6	2014-06-05	900	N,w,M	QSO	0.078
J174526.95+020532.6	2FGL J1745.6+0203	17:45:26.96	+02:05:32.8	2014-06-05	1200	w,M	QSO	0.335
J183535.34+134848.8	2FGL J1835.4+1349	18:35:35.35	+13:48:48.8	2014-06-05	600	V,T,N,87,rf,w,M,U	BL Lac	?
J025333.64+321720.8	2FGL J0253.4+3218	02:53:33.64	+32:17:20.9	2014-02-22	600	N,87,GB,c,rf,w	QSO	0.859
J074642.31-475455.0	2FGL J0746.5-4758	07:46:42.31	-47:54:55.2	2014-04-23	600	Pm,S,A,c,rf,w,M	BL Lac	?
J084502.48-545808.4	2FGL J0844.8-5459	08:45:02.47	-54:58:08.6	2014-04-23	600	Pm,A,rf,U,X	BL Lac	?
J085654.85+714623.8	2FGL J0856.0+7136	08:56:54.86	+71:46:23.9	2014-02-22	600	W,N,87,GB,c,rf,w,M,g,X	QSO	0.542
J114141.80-140754.6	2FGL J1141.7-1404	11:41:41.84	-14:07:53.5	2014-04-23	900	L,Pm,N,c,w,M,U	BL Lac	?
J123824.39-195913.8	2FGL J1238.1-1953	12:38:24.40	-19:59:13.5	2014-04-23	900	Pm,N,A,c,rf,w,M,g,X	BL Lac	?
J140609.60-250809.2	2FGL J1406.2-2510	14:06:09.60	-25:08:09.3	2014-04-23	600	L,N,w,M,U,u,x - SED in Takeuchi+13	BL Lac	?
J162638.15-763855.5	2FGL J1626.0-7636	16:26:38.18	-76:38:55.5	2014-04-23	300	Pm,S,c,rf,w,M,g	BL Lac	0.1050
J184931.74+274800.8	2FGL J1849.5+2744	18:49:31.69	+27:48:00.9	2014-06-04	1800	W,N,87,c,rf,w,M	BL Lac	?
J195945.66-472519.3	2FGL J1959.9-4727	19:59:45.68	-47:25:19.3	2014-04-23	600	S,w,M,U,g,u,X,x - SED in Takeuchi+13	BL Lac	≥ 0.519
J024440.30-581954.5	BZBJ0244-5819	02:44:40.31	-58:19:54.6	2014-02-03	600	BL Lac candidate at $z=0.265$	BL Lac	≥ 0.265
J121752.08+300700.6	BZBJ1217+3007*	12:17:52.09	+30:07:00.7	2014-06-04	300	BL Lac at $z=0.13?$	BL Lac	?
J135949.71-374600.7	BZBJ1359-3746*	13:59:49.72	-37:46:00.8	2014-04-23	300	BL Lac	BL Lac	?
J155333.56-311830.9	BZBJ1553-3118*	15:53:33.56	-31:18:31.0	2014-04-23	300	BL Lac ($z=0.132$ -BL Lac-Masetti+13)	BL Lac	?
J164924.98+523515.0	BZBJ1649+5235*	16:49:25.00	+52:35:15.0	2014-06-05	900	BL Lac candidate at $z=?$	BL Lac	?
J170209.63+264314.7	BZBJ1702+2643	17:02:09.64	+26:43:14.8	2014-06-05	1200	BL Lac candidate at $z=?$	BL Lac	?
J180945.39+291019.8	BZBJ1809+2910*	18:09:45.39	+29:10:20.0	2014-06-05	900	BL Lac candidate at $z=?$	BL Lac	?
J203923.51+521950.1	BZBJ2039+5219*	20:39:23.50	+52:19:49.9	2014-06-04	600	BL Lac candidate at $z=0.053$	BL Lac	?

Their redshifts are reported in Table 1.

4.2. Gamma-ray Active Galaxies of Uncertain type

In this subsection we discuss the AGUs in our observed sample. The multifrequency notes relative to each source are reported in Table 1, as previously done for the UGSs. The spectra of the whole AGU sample are shown in Figure 13-22. Our spectroscopic observations confirm that 8 out of 10 sources are BL Lac objects while the remaining two, having quasar-like optical spectra and flat radio spectra, are indeed BZQs. The optical spectra of these two BZQs, *WISE* J025333.64+321720.8 and *WISE* J085654.85+714623.8, contain broad emission lines identified as Mg II and H β (see Figures 13 and 16 for more details), and permit us to measure their redshifts of 0.859 and 0.542, respectively. In particular, the identifications of [OII], H β and [OIII] doublet in the optical spectrum of *WISE* J025333.64+321720.8 are uncertain due to low SNR. The optical spectrum of *WISE* J084502.48-545808.4, candidate counterpart of 2FGL J0844.8-5459, show an absorption feature ($\lambda_{obs} = 6364 \text{ \AA}$ with $EW_{obs} = 2.2 \text{ \AA}$) that we are not able to clearly identify (see Figure 15). We classify the *WISE* J162638.15-763855.5 counterpart to 2FGL J1626.0-

7636 as a BL Lac since its emission lines have $EW < 5 \text{ \AA}$. The detection of emission ([O I] with $EW_{obs} = 2.3 \text{ \AA}$, the [S II] doublet $\lambda\lambda_{obs} = 7421 - 7438 \text{ \AA}$ with $EW_{obs} = 2.5 - 2.4 \text{ \AA}$) and absorption lines (G band, Mg I with $EW_{obs} = 4.9 \text{ \AA}$ and Na I with $EW_{obs} = 3.3 \text{ \AA}$), enable us to measure a redshift of 0.1050 (see Figure 20). The optical spectra of the AGUs associated with the γ -ray source 2FGL J1849.5+2744 are also published in Shaw et al. (2013a). The source is listed as a BZB in the 2LAC catalog, although the optical spectrum was not yet available. The optical spectrum collected by us for this object (*WISE* J184931.74+274800.8) is nearly featureless (see Figure 21), so we are not able to confirm the lower limit z estimate (i.e., 1.466) of this source proposed by Shaw et al. (2013a) on the basis of Mg II absorption doublet. Thanks to our optical spectrum of the *WISE* J195945.66-472519.3, candidate counterpart to 2FGL J1959.9-4727, we can put a lower limit on its redshift of 0.519 based on the detection of an intervening doublet system of Mg II ($\lambda\lambda_{obs} = 4246 - 4256 \text{ \AA}$ with $EW_{obs} = 1.4 - 0.9 \text{ \AA}$; see also Figure 22).

4.3. BL Lac objects

Details for the BL Lacs in our sample are listed below. Table 1 reports their Roma-BZCAT name and

the name of the *WISE* counterpart with the coordinates. Multifrequency notes are not presented in this table since they are already extensively discussed in the Roma-BZCAT. All the BZBs that are also detected by *Fermi* belong to the sample named: *locus* (i.e. the three-dimensional region in the *WISE* color space occupied by the γ -ray-emitting blazars, well separated from the regions occupied by other classes, D’Abrusco et al. 2013), with the only exception being BZB J2039+5219. They were used in D’Abrusco et al. (2013) to build the method to search for blazar-like sources within the positional uncertainty region of the *Fermi* UGSs. Thus all their *WISE* counterparts have the IR colors consistent with the *Fermi* blazar population. There are five objects listed in Table 1 as BL Lac candidates for which no optical spectra are present in literature that allowed a firm classification. Our spectroscopic observations confirmed that all the BL Lac candidates have featureless optical spectra as shown in Figures 23-30. In addition, the remaining three objects, namely BZB J1217+3007, BZB J1359-3746 and BZB J1553-3118, that were indeed classified BZBs with an uncertain redshift estimate when the Roma-BZCAT was released. For one BZB, BZB J0244-5819, we have been able to estimate a lower limit on its redshift, $z \geq 0.265$, on the basis of absorption features in its optical spectrum. Our observation of *WISE* J024440.30-581954.5 show the doublet Ca H+K ($\lambda_{obs} = 4975 - 5017 \text{ \AA}$ with $EW_{obs} = 0.7 - 1 \text{ \AA}$), G band, Mg I ($EW_{obs} = 1.5 \text{ \AA}$) and Na I ($EW_{obs} = 1.1 \text{ \AA}$) absorption features that could be due to the host galaxy and/or to intervening systems (see Figure 23). We note that BZB J1359-3746, BZB J1649+5235 and BZB J1809+2910 also have published optical spectra for their candidate counterparts released in Shaw et al. (2013b). In addition, Shaw et al. (2013b) reported the spectrum of BZB J1359-3746, with the detection of the Calcium break that allowed them to determine a redshift of 0.334. We cannot confirm this result since our optical spectrum of *WISE* J135949.71-374600.7 shows a featureless continuum (see Figure 25). We also present the spectrum of the low-energy counterpart of BZB J1553-3118, which was also published in Masetti et al. (2013) with a redshift of 0.132. In our lower signal to noise observation, its IR counterpart *WISE* J135949.71-374600.7 appears featureless, as shown in Figure 26. The optical spectrum of *WISE* J203923.51+521950.1, candidate counterpart of BZB J2039+5219, show an absorption feature at $\lambda_{obs} = 6212 \text{ \AA}$ with $EW_{obs} = 4.8 \text{ \AA}$. We do not have

a clear identification for this feature (see also Figure 30).

5. Summary and conclusions

We present here the results of our 2014 spectroscopic campaign carried out in the Northern hemisphere with the KPNO and Palomar telescopes, and in the Southern hemisphere with the SOAR and Magellan telescopes. The main goal of our campaign is to confirm the nature of sources selected for having IR colors or low radio frequency spectra (i.e., below $\sim 1\text{GHz}$) similar to known *Fermi*-detected blazars and lying within the positional uncertainty regions of the UGSs through optical spectroscopic observations. Given the positional uncertainty of the UGSs, there could be a possible contamination by different source classes in these selection procedures of γ -ray blazar candidates (e.g., Stern & Assef 2013) and spectroscopic observations are the only way to remove such degeneracy (e.g., Masetti et al. 2013; Shaw et al. 2013a; Shaw et al. 2013b; Paggi et al. 2014; Massaro et al. 2014a) and discover new gamma-ray blazars. The confirmation of the blazar nature of these selected objects will improve/refine future associations for the *Fermi* catalog and will also yield to understand the efficiency and completeness of the association method based on the *WISE* colors once our campaign is completed. Our spectroscopic observations could potentially allow us to obtain redshift estimates for the UGS candidate counterparts. During our campaign we also observed several AGUs, as defined according to the *Fermi* catalogs (see e.g., Ackermann et al. 2011a; Nolan et al. 2012), to verify if they are indeed blazars. In addition we observed several sources that already belong to the Roma-BZCAT but were classified as BL Lac candidates due to the lack of optical spectra available in literature, or were BL Lac objects with uncertain redshift estimates, when the Roma-BZCAT v4.1 was released.

We observed a total of 27 targets. The results of this spectroscopic campaign are reported as follows:

- In the sample of potential counterparts for the UGS, selected based on their IR colors (Massaro et al. 2011a; D’Abrusco et al. 2013; Massaro et al. 2013a) and on the basis of their flat radio spectra below $\sim 1 \text{ GHz}$ (Massaro et al. 2013b; Nori et al. 2014; Massaro et al. 2014b), we confirm the blazar nature of 8 of 9 UGSs. Among them, six are clearly BL Lacs presenting fea-

tureless optical spectra. The remaining two are QSOs. One potential counterparts for 2FGL J1745.6+0203 found on the basis of the IR color selection method, namely *WISE* J174526.95+020532.6, is a QSO that probably contaminates our selection method.

- We classify *WISE* J173052.85-035247.2 as a BL Lac although this source is not associated with any NVSS counterpart, as expected for BL Lac objects. The detection of an intervening doublet system of Mg II enabled us to set a lower limit on its redshift of 0.776.
- All the sources that belong to our AGU subsample have a blazar nature. Two of them are QSOs, while for one of them, namely *WISE* J162638.15-763855.5, we have been able to detect some features in the optical spectrum, both in emission and in absorption, leading to a redshift measurement of 0.1050. The AGU associated with the *WISE* J184931.74+274800.8 has been classified as a BZB in the 2LAC paper but at that time there was no optical spectra. Our observations confirm its BL Lac nature. We have been also able to set a lower limit for the AGU associated with *WISE* J195945.66-472519.3 of 0.519 thanks to the detection in its optical spectrum of a Mg II intervening system.
- Within the Roma-BZCAT sources we found five BL Lac candidates that thanks to the collected optical spectra are all confirmed BL Lacs. For one of them, BZB J0244-5819, we have been able to set a lower limit on their redshifts on the basis of absorption systems (Ca H+K, G band, Mg I and Na I) that could be due to the host galaxy and/or to intervening systems. For the remaining four BZBs listed in the Roma-BZCAT with uncertain redshift estimates, we were not able to obtain any redshift values.

We are grateful to Dr. D. Hammer and Dr. S. Points for their help to schedule, prepare and perform the KPNO and the SOAR observations, respectively. We are grateful to F. La Franca for the fruitful discussions that significantly improved the paper. This investigation is supported by the NASA grants NNX12AO97G and NNX13AP20G. F. Ricci acknowledges the grants MIUR PRIN 2010-2011 and INAF-PRIN 2011. H. A. Smith acknowledges partial support from NASA/JPL

grant RSA 1369566. The work by G. Tosti is supported by the ASI/INAF contract I/005/12/0. Part of this work is based on archival data, software or on-line services provided by the ASI Science Data Center. This research has made use of data obtained from the high-energy Astrophysics Science Archive Research Center (HEASARC) provided by NASA's Goddard Space Flight Center; the SIMBAD database operated at CDS, Strasbourg, France; the NASA/IPAC Extragalactic Database (NED) operated by the Jet Propulsion Laboratory, California Institute of Technology, under contract with the NASA. Part of this work is based on the NVSS (NRAO VLA Sky Survey): the National Radio Astronomy Observatory is operated by Associated Universities, Inc., under contract with the National Science Foundation and on the VLA low-frequency Sky Survey (VLSS). The Molonglo Observatory site manager, D. Campbell-Wilson, and the staff, J. Webb, M. White and J. Barry, are responsible for the smooth operation of Molonglo Observatory Synthesis Telescope (MOST) and the day-to-day observing programme of SUMSS. The SUMSS survey is dedicated to M. Large whose expertise and vision made the project possible. The MOST is operated by the School of Physics with the support of the Australian Research Council and the Science Foundation for Physics within the University of Sydney. This publication makes use of data products from the *Wide-field Infrared Survey Explorer*, which is a joint project of the University of California, Los Angeles, and the Jet Propulsion Laboratory/California Institute of Technology, funded by NASA. This publication makes use of data products from the Two Micron All Sky Survey, which is a joint project of the University of Massachusetts and the Infrared Processing and Analysis Center/California Institute of Technology, funded by NASA and NSF. This research has made use of the USNOFS Image and Catalogue Archive operated by the United States Naval Observatory, Flagstaff Station⁷. Funding for the SDSS and SDSS-II has been provided by the Alfred P. Sloan Foundation, the Participating Institutions, the NSF, the U.S. Department of Energy, NASA, the Japanese Monbukagakusho, the Max Planck Society, and the Higher Education Funding Council for England. The SDSS Web Site is <http://www.sdss.org/>. The SDSS is managed by the Astrophysical Research Consortium for the Participating Institutions. The Participating Institutions are the

⁷<http://www.nofs.navy.mil/data/fchpix/>

American Museum of Natural History, Astrophysical Institute Potsdam, University of Basel, University of Cambridge, Case Western Reserve University, University of Chicago, Drexel University, Fermilab, the Institute for Advanced Study, the Japan Participation Group, Johns Hopkins University, the Joint Institute for Nuclear Astrophysics, the Kavli Institute for Particle Astrophysics and Cosmology, the Korean Scientist Group, the Chinese Academy of Sciences (LAMOST), Los Alamos National Laboratory, the Max-Planck-Institute for Astronomy (MPIA), the Max-Planck-Institute for Astrophysics (MPA), New Mexico State University, Ohio State University, University of Pittsburgh, University of Portsmouth, Princeton University, the United States Naval Observatory, and the University of Washington. The WENSS project was a collaboration between the Netherlands Foundation for Research in Astronomy and the Leiden Observatory. We acknowledge the WENSS team consisted of G. de Bruyn, Y. Tang, R. Rengelink, G. Miley, H. Röttgering, M. Bremer, M. Bremer, W. Brouw, E. Raimond and D. Fullagar for the extensive work aimed at producing the WENSS catalog. TOPCAT⁸ (Taylor 2005) for the preparation and manipulation of the tabular data and the images. The Aladin Java applet⁹ was used to create the finding charts reported in this paper (Bonnarel et al. 2000). It can be started from the CDS (Strasbourg, France), from the CFA (Harvard, USA), from the ADAC (Tokyo, Japan), from the IUCAA (Pune, India), from the UKADC (Cambridge, UK), or from the CADC (Victoria, Canada).

REFERENCES

- Abdo, A. A., Ackermann, M., Ajello, M. et al. 2010 *ApJS*, 188, 405
- Abdo A. A., et al., 2014, in preparation
- Ackermann, M., Ajello, M., Allafort, A. et al. 2011a *ApJ*, 743, 171
- Ackermann, M. et al. 2011b *ApJ*, 741, 30
- Ackermann, M., Ajello, M., Allafort, A. et al. 2012 *ApJ*, 753, 83
- Acero, F., Donato, D., Ojha, R. et al. 2013 *ApJ*, 779, 133
- Ahn, C. P., Alexandroff, R., Allende Prieto, C. et al. 2012, *ApJS*, 203, 21
- Bigelow, B. C., Dressler, A. M., Shectman, S. A., & Epps, H. W. 1998, in *Society of Photo-Optical Instrumentation Engineers (SPIE) Conference Series*, Vol. 3355, *Society of Photo-Optical Instrumentation Engineers (SPIE) Conference Series*, ed. S. D’Odorico, 225
- Bonnarel, F., Fernique, P., Bienaymé, O., Egret, D., Genova, F., Louys, M., Ochsenein, F., Wenger, M., Bartlett, J. G., 2000, *A&AS*, 143, 33
- Blandford, R. D., Rees, M. J., 1978, *PROC. "Pittsburgh Conference on BL Lac objects"*, 328
- Cardelli, J. A., Clayton, G. C., & Mathis, J. S. 1989, *ApJ*, 345, 245
- Cohen, A. S., Lane, W. M., Cotton, W. D. et al. 2007 *AJ*, 134, 1245
- Condon, J. J., Cotton, W. D., Greisen, E. W. et al. 1998, *AJ*, 115, 1693
- Cutri et al. 2012 wise.rept, 1C
- D’Abrusco, R., Massaro, F., Ajello, M., Grindlay, J. E., Smith, Howard A. & Tosti, G. 2012 *ApJ*, 748, 68
- D’Abrusco, R., Massaro, F., Paggi, A. et al. 2013 *ApJS*, 206, 12
- Doert, M. & Errando, M. 2014 *ApJ*, 782, 41
- Evans, I. N., Primini, F. A., Glotfelty, K. J. et al. 2010 *ApJS*, 189, 37
- Evans, P. A., Osborne, J. P., Beardmore, A. P. et al. 2014 *ApJS*, 210, 8
- Ghirlanda, G. et al. 2010 *MNRAS*, 407, 791
- Hassan, T., Mirabal, N., Contreras, J. L., Oya, I. 2013 *MNRAS*, 428, 220
- Healey, S. E., Romani, R. W., Taylor, G. B. et al. 2007 *ApJS*, 171, 61
- Horne, K. 1986, *PASP*, 98, 609
- Jones, H. D. et al. 2004 *MNRAS*, 355, 747
- Jones, H. D. et al. 2009 *MNRAS*, 399, 683

⁸<http://www.star.bris.ac.uk/~mbt/topcat/>

⁹<http://aladin.u-strasbg.fr/aladin.gml>

- Kovalev, Y. Y. 2009 ApJ, 707L, 56
- Lane, W. M., Cotton, W. D., van Velzen, S. et al. 2014 MNRAS, 440, 327
- Laurent-Muehleisen, S.A. et al., 1999, ApJ, 525, 127
- Londish D., Heidt J., Boyle B. J., Croom S. M., Kedziora-Chudczer L., 2004, MNRAS, 352, 903
- Mahony, E. K. et al. 2010 ApJ, 718, 587
- Masetti, N., Sbarufatti, B., Parisi, P. 2013 A&A, 559A, 58
- Massaro, E., Giommi, P., Leto, C. et al. 2009 A&A, 495, 691
- Massaro, F., D’Abrusco, R., Ajello, M., Grindlay, J. E. & Smith, H. A. 2011a ApJ, 740L, 48
- Massaro, E., Giommi, P., Leto, C. et al. 2011b “Multifrequency Catalogue of Blazars (3rd Edition)”, ARACNE Editrice, Rome, Italy
- Massaro, F., D’Abrusco, R., Tosti, G., Ajello, M., Paggi, A., Gasparrini, 2012a ApJ, 752, 61
- Massaro, F., D’Abrusco, R., Tosti, G., Ajello, M., Gasparrini, D., Grindlay, J. E. & Smith, Howard A. 2012b ApJ, 750, 138
- Massaro, F., D’Abrusco, R., Paggi, A., Tosti, G., Gasparrini, D. 2012c ApJ, 750L, 35
- Massaro, F., D’Abrusco, R., Paggi, A. et al. 2013a ApJS, 206, 13
- Massaro, F., D’Abrusco, R., Giroletti, M. et al. 2013b ApJS, 207, 4
- Massaro, F., Masetti, N., D’Abrusco, R. et al. 2014a AJ in press
- Massaro, F., Giroletti, M., D’Abrusco, R. et al. 2014b ApJS, 213, 3
- Mauch, T., Murphy, T., Buttery, H. J. et al. 2003 MNRAS, 342, 1117
- Mirabal, N. 2009 ApJ, 701, 129
- Mirabal, N.; Frías-Martínez, V.; Hassan, T.; Frías-Martínez, E. 2012 MNRAS, 424L, 64
- Monet, D. G. et al. 2003 AJ, 125, 984
- Murphy, T. et al. 2010 MNRAS, 402, 2403
- Nolan, P. L., Abdo, A. A., Ackermann, M. et al. 2012 ApJS, 199, 31
- Nori, M., Giroletti, M., Massaro, F., D’Abrusco, R., Paggi, A. & Tosti, G. et al. 2014 ApJS 212, 3
- Paggi, A., Massaro, F., D’Abrusco, R. et al. 2013 ApJS, 209, 9
- Paggi, A., Milisavljevic, D., Masetti, N. et al. 2014 AJ, 147, 112
- Petrov, L., Mahony, E. K., Edwards, P. G. et al. 2013 MNRAS, 432, 1294
- Rengelink, R., Tang, Y., de Bruyn, A. G. et al. 1997, A&A Suppl. 124, 259
- Saxton, R. D. 2008 A&A, 480, 611
- Schlegel, D. J., Finkbeiner, D. P., & Davis, M. 1998, ApJ, 500, 525
- Shaw, M. S., Romani, R. W.; Cotter, G. et al. 2013 ApJ, 764, 135
- Shaw, M. S., Filippenko, A. V., Romani, R. W. et al. 2013 AJ, 146, 127
- Stern, D. & Assef, R. J. 2013 ApJ, 764L, 30
- Skrutskie, M. F. et al. 2006, AJ, 131, 1163
- Stickel, M. et al. 1991 ApJ, 374, 431
- Stoeckel et al. 1991, ApJS, 76, 813
- Stroh, M. C. & Falcone, A. D. 2013, ApJS, 207, 28
- Takeuchi, Y., Kataoka, J., Maeda, K. et al. 2013 ApJS, 208, 25
- Taylor, M. B. 2005, ASP Conf. Ser., 347, 29
- Tody, D. 1986 SPIE, 627, 733
- Urry, C. M., & Padovani, P. 1995, PASP, 107, 803
- Voges, W. et al. 1999 A&A, 349, 389
- Voges, W. et al. 2000 IAUC, 7432R, 1.
- Warwick, R. S.; Saxton, R. D.; Read, A. M. 2012 A&A, 548A, 99
- Wright, A. & Otrupcek, R. 1990 PKS, C, 0
- Wright, A. E., Griffith, M. R., Burke, B. F., Ekers, R. D. 1994 ApJS, 91, 111

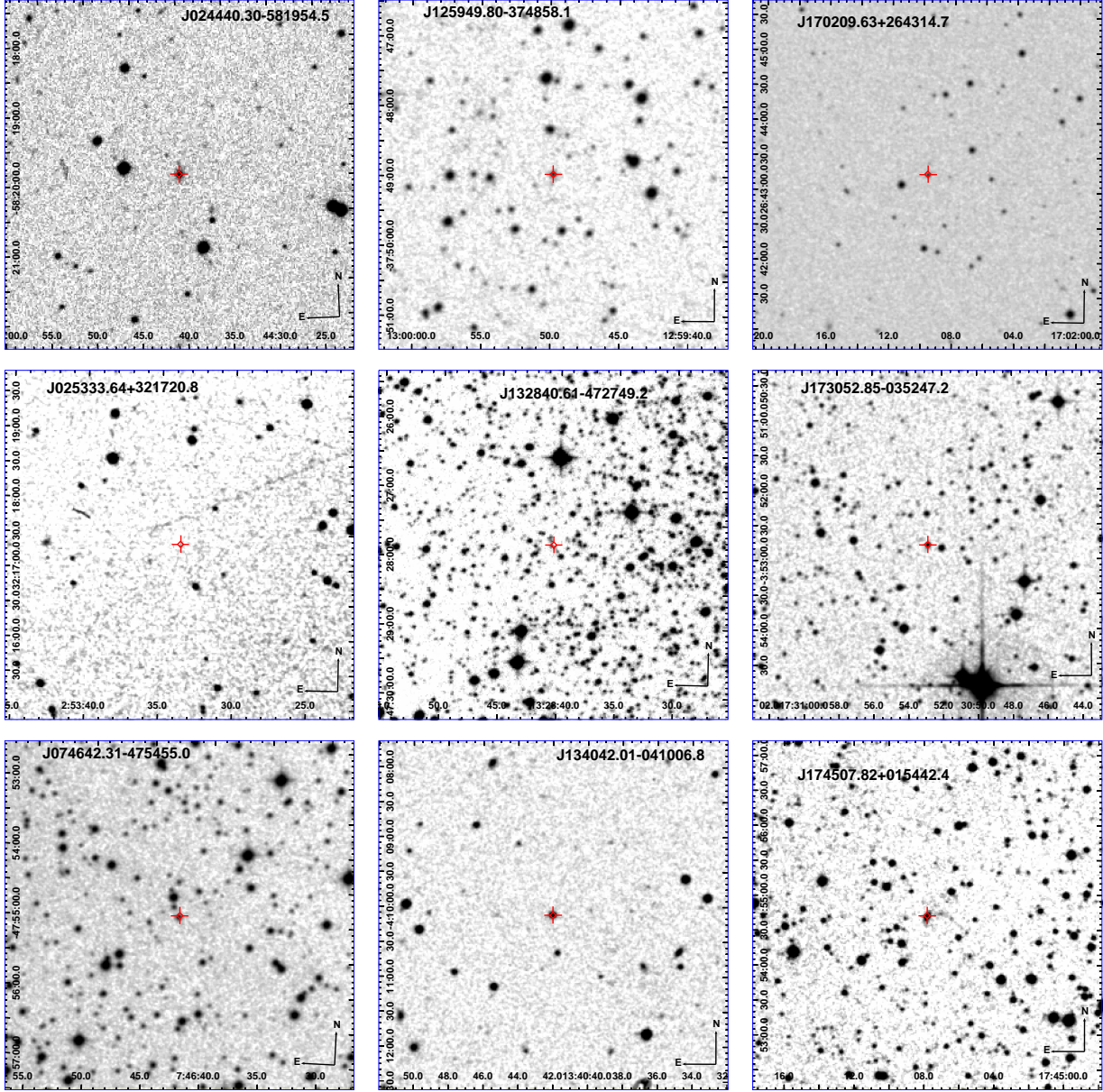


Fig. 1.— Optical images, $5'$ on a side, of 9 of the *WISE* sources selected in this paper for optical spectroscopic follow-up. The proposed optical counterparts are indicated with red marks and the fields are extracted from the DSS-II-Red survey. Object name, image scale and orientation are also reported in each panel.

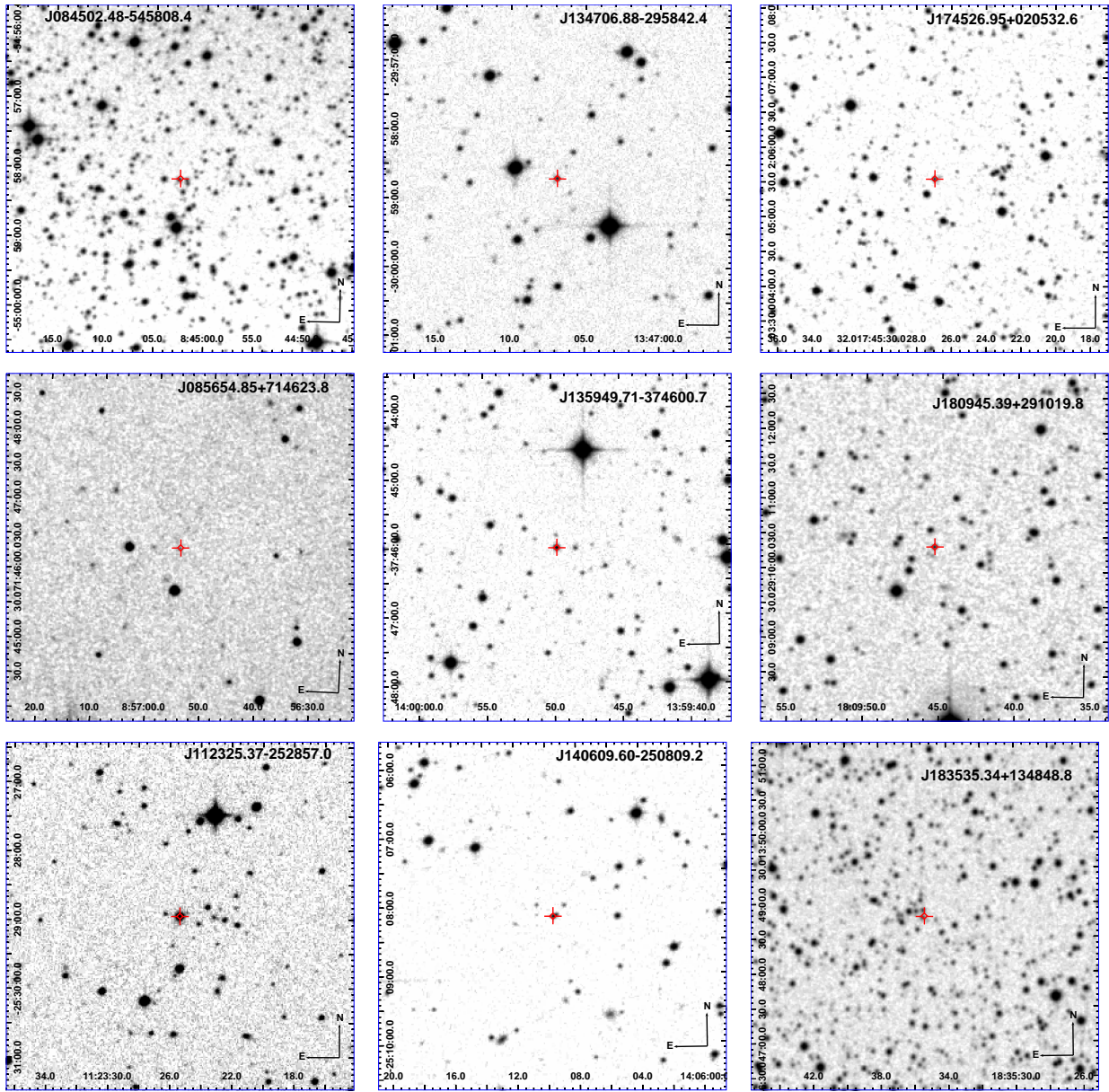


Fig. 2.— Same as Figure 1.

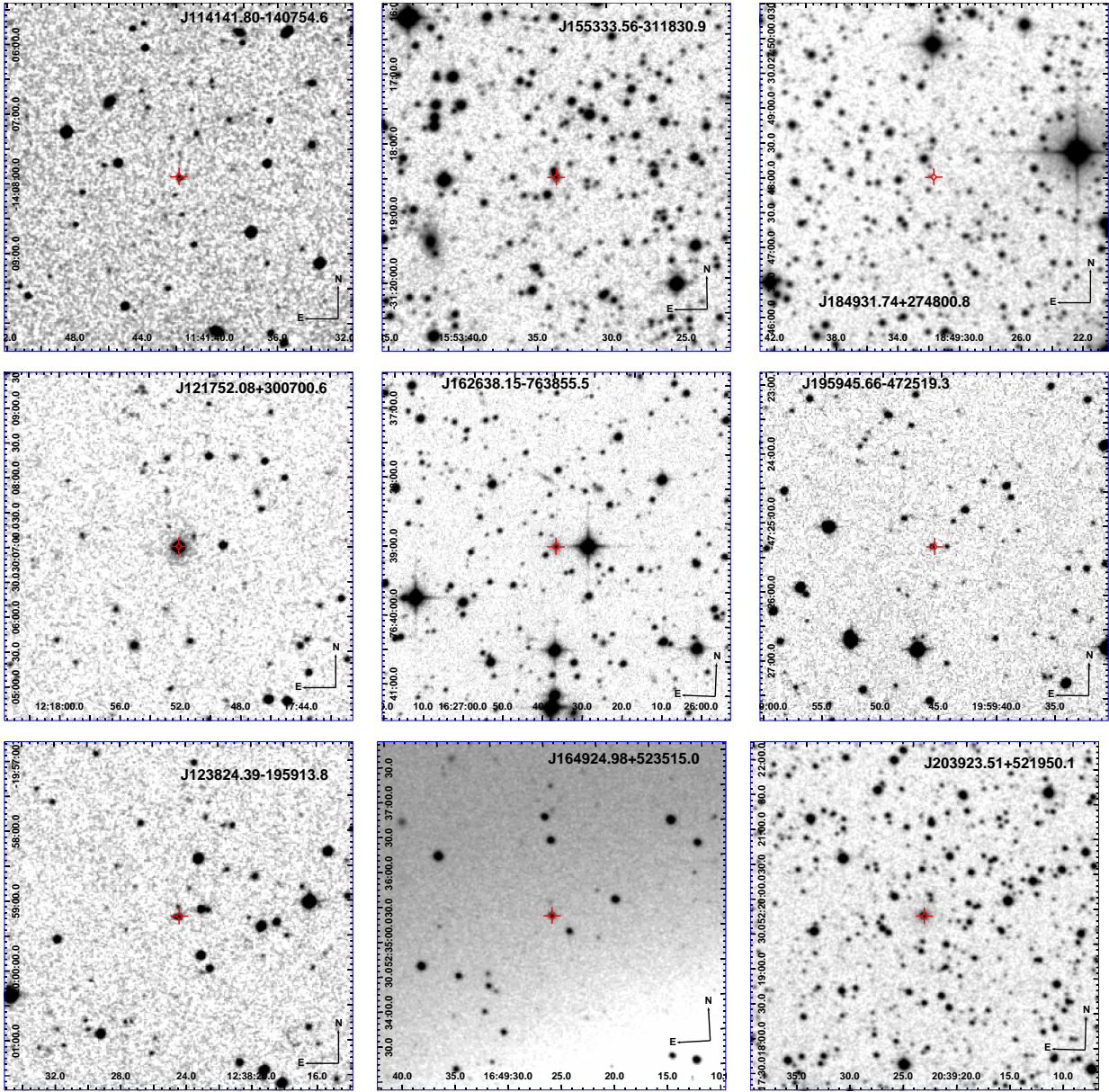


Fig. 3.— Same as Figure 1.

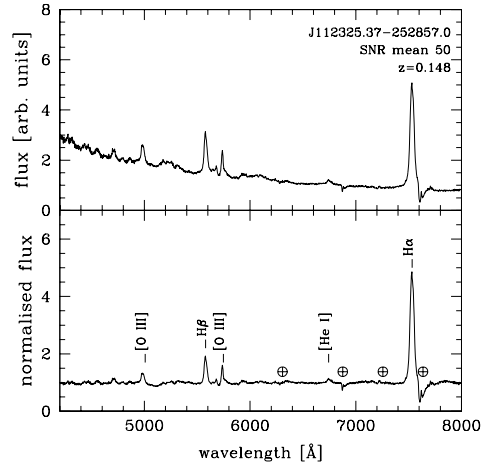


Fig. 4.— Upper panel: optical spectra observed at SOAR of *WISE* J112325.37-252857.0, potential counterpart associated with 2FGL J1123.3-2527, classified as a QSO at $z=0.148$ on the basis of the identification of the emission lines shown in the spectra. The average SNR is also reported in the figure. Lower panel: the normalised spectrum is shown. The symbol \oplus indicates atmospheric telluric features.

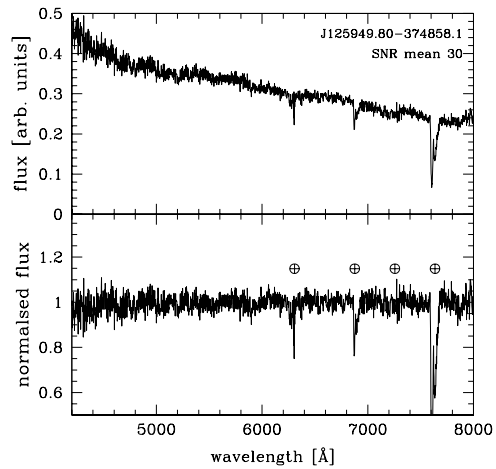


Fig. 5.— Upper panel: optical spectra observed at SOAR of *WISE* J125949.80-374858.1, potential counterpart associated with FGL J1259.8-3749, classified as a BL Lac on the basis of its featureless continuum. Lower panel: as in Figure 4.

This 2-column preprint was prepared with the AAS L^AT_EX macros v5.2.

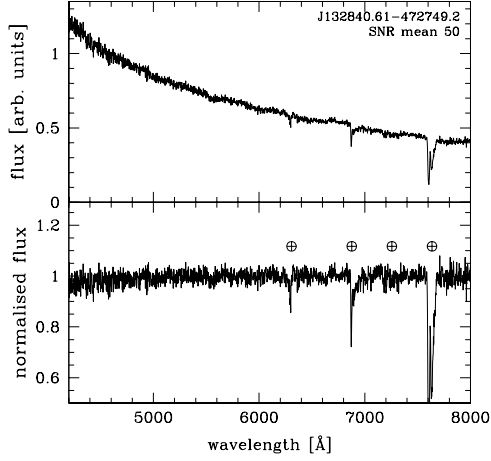


Fig. 6.— Upper panel: optical spectra observed at SOAR of *WISE* J132840.61-472749.2, potential counterpart associated with 2FGL J1328.5-4728, classified as a BL Lac on the basis of its featureless continuum. Lower panel: as in Figure 4.

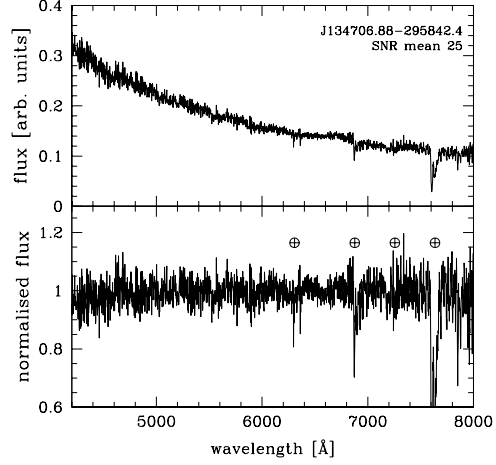


Fig. 8.— Upper panel: optical spectra observed at SOAR of *WISE* J134706.88-295842.4, potential counterpart associated with 2FGL J1347.0-2956, classified as a BL Lac on the basis of its featureless continuum. Lower panel: as in Figure 4.

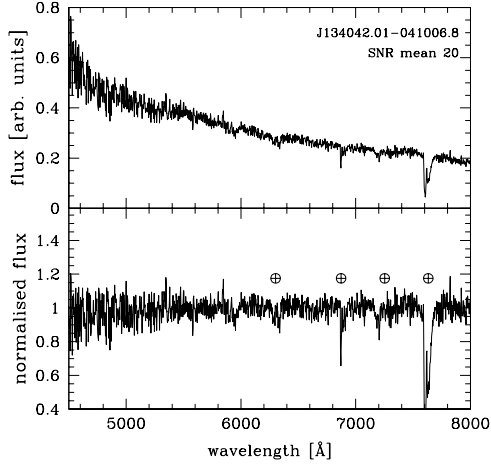


Fig. 7.— Upper panel: optical spectra observed at KPNO of *WISE* J134042.01-041006.8, potential counterpart associated with 2FGL J1340.5-0412, classified as a BL Lac on the basis of its featureless continuum. Lower panel: as in Figure 4.

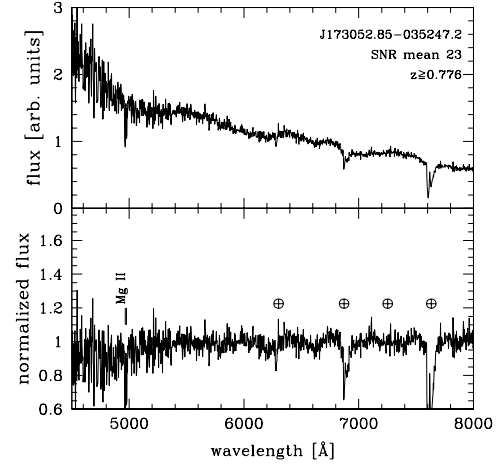


Fig. 9.— Upper panel: optical spectra observed at KPNO of *WISE* J173052.85-035247.2, potential counterpart associated with 2FGL J1730.6-0353, classified as a BL Lac on the basis of its featureless continuum. Lower panel: as in Figure 4.

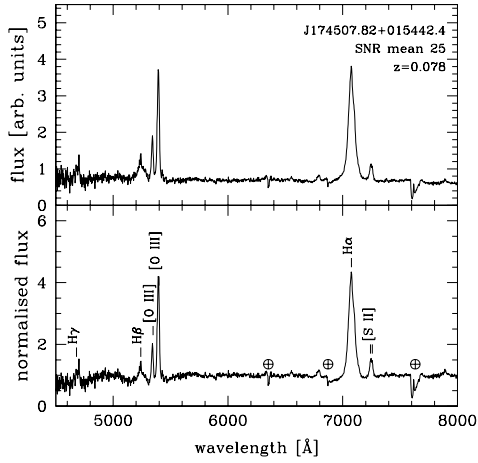


Fig. 10.— Upper panel: optical spectra observed at KPNO of *WISE* J174507.82+015442.4, potential counterpart associated with 2FGL J1745.6+0203, classified as a QSO at $z=0.078$ on the basis of the identification of the emission lines visible in the spectra. Lower panel: as in Figure 4.

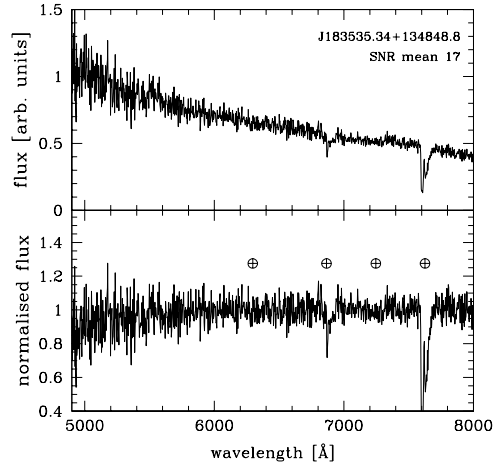


Fig. 12.— Upper panel: optical spectra observed at KPNO of *WISE* J183535.34+134848.8, potential counterpart associated with 2FGL J1835.4+1349, classified as a BL Lac on the basis of its featureless continuum. Lower panel: as in Figure 4.

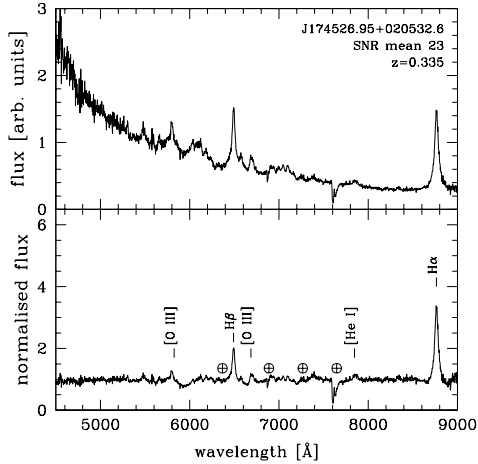


Fig. 11.— Upper panel: optical spectra observed at KPNO of *WISE* J174526.95+020532.6, potential counterpart associated with 2FGL J1745.6+0203, classified as a QSO at $z=0.335$ on the basis of the identification of the emission lines visible in the spectra. Lower panel: as in Figure 4.

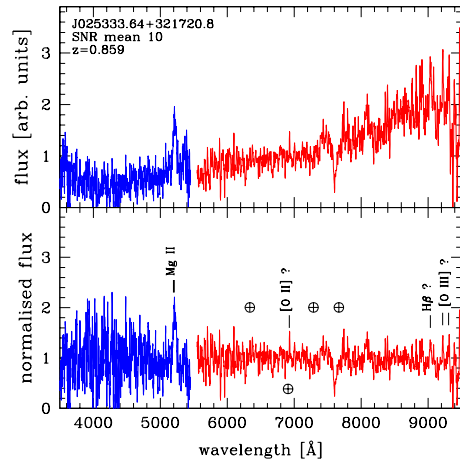


Fig. 13.— Upper panel: optical spectra observed at Palomar of *WISE* J025333.64+321720.8, potential counterpart associated with 2FGL J0253.4+3218, classified as a QSO at $z=0.859$ on the basis of the identification of the emission lines listed on the spectra. Red and blue spectra show the two sides of the dual-beam spectrograph. Lower panel: as in Figure 4.

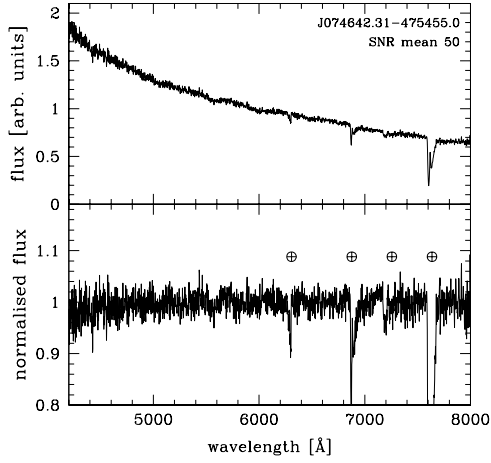


Fig. 14.— Upper panel: optical spectra observed at SOAR of *WISE* J074642.31-475455.0, potential counterpart associated with 2FGL J0746.5-4758, classified as a BL Lac on the basis of its featureless continuum. Lower panel: as in Figure 4.

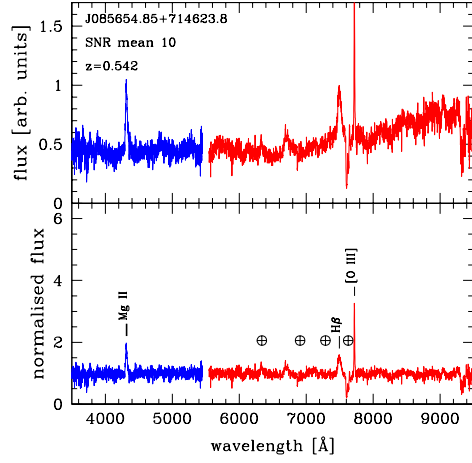


Fig. 16.— Upper panel: optical spectra observed at Palomar of *WISE* J085654.85+714623.8, potential counterpart associated with 2FGL J0856.0+7136, classified as a QSO at $z=0.542$ on the basis of the identification of the emission lines visible in the spectra. Red and blue spectra show the two sides of the dual-beam spectrograph. Lower panel: as in Figure 4.

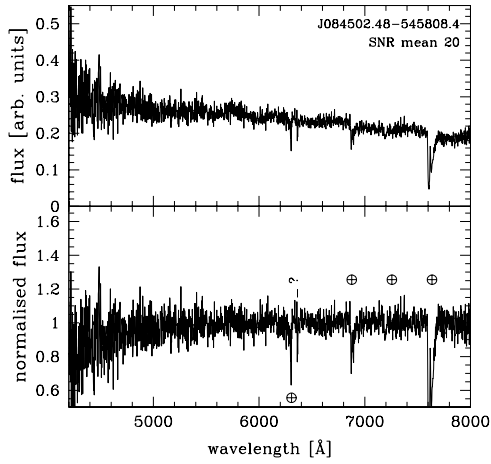


Fig. 15.— Upper panel: optical spectra observed at SOAR of *WISE* J084502.48-545808.4, potential counterpart associated with 2FGL J0844.8-5459, classified as a BL Lac on the basis of its featureless continuum. Lower panel: as in Figure 4.

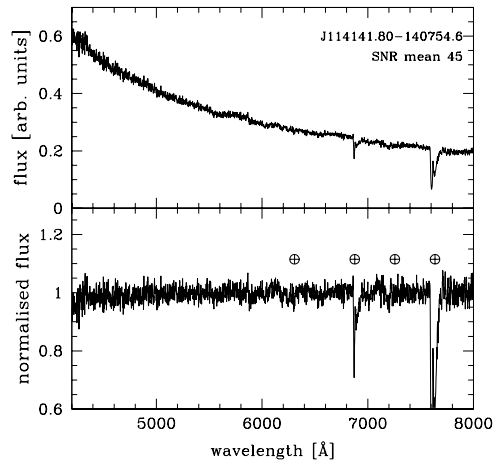


Fig. 17.— Upper panel: optical spectra observed at SOAR of *WISE* J114141.80-140754.6, potential counterpart associated with 2FGL J1141.7-1404, classified as a BL Lac on the basis of its featureless continuum. Lower panel: as in Figure 4.

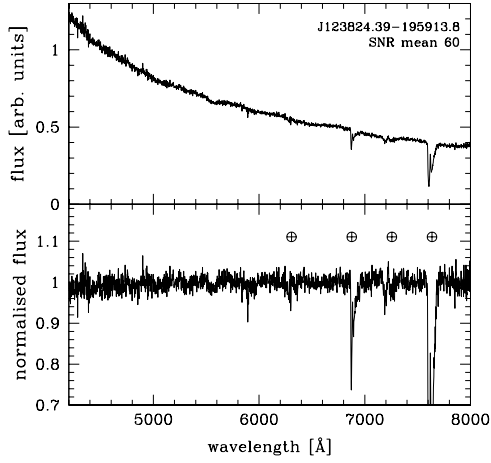


Fig. 18.— Upper panel: optical spectra observed at SOAR of *WISE* J123824.39-195913.8, potential counterpart associated with 2FGL J1238.1-1953 classified as a BL Lac on the basis of its featureless continuum. Lower panel: as in Figure 4.

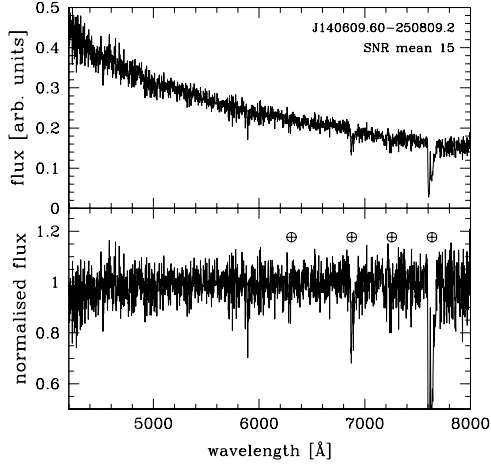


Fig. 19.— Upper panel: optical spectra observed at SOAR of *WISE* J140609.60-250809.2, potential counterpart associated with 2FGL J1406.2-2510, classified as a BL Lac on the basis of its featureless continuum. Lower panel: as in Figure 4.

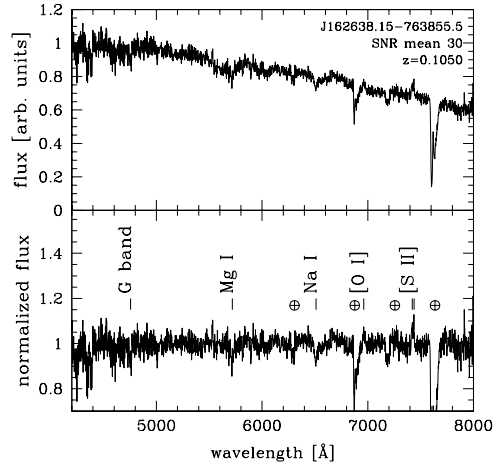


Fig. 20.— Upper panel: optical spectra observed at SOAR of *WISE* J162638.15-763855.5, potential counterpart associated with 2FGL J1626.0-7636, classified as a BL Lac since its emission and absorption lines have $EW \lesssim 5 \text{ \AA}$. The detection of emission ([O I] and the [S II] doublet) and absorption lines (G band, Mg I and Na I) has enabled us to estimate a redshift of 0.1050. Lower panel: as in Figure 4.

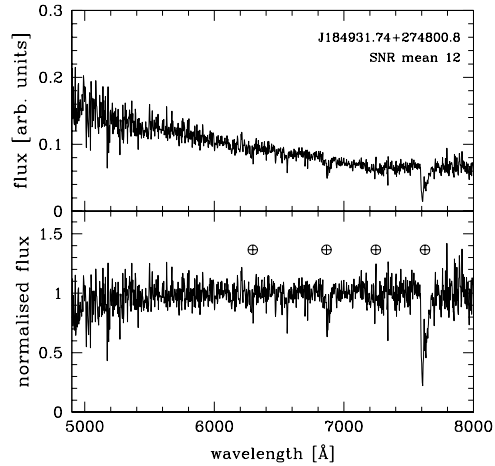


Fig. 21.— Upper panel: optical spectra observed at KPNO of *WISE* J184931.74+274800.8, potential counterpart associated with 2FGL J1849.5+2744, classified as a BL Lac on the basis of its featureless continuum. Lower panel: as in Figure 4.

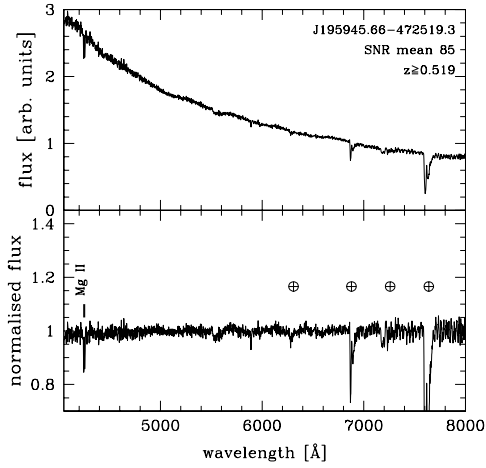


Fig. 22.— Upper panel: optical spectra observed at SOAR of *WISE* J195945.66-472519.3, potential counterpart associated with 2FGL J1959.9-4727, classified as a BL Lac on the basis of its featureless continuum. Lower panel: as in Figure 4.

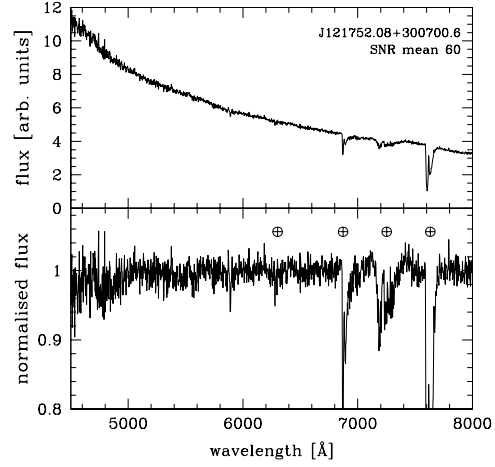


Fig. 24.— Upper panel: optical spectra observed at KPNO of *WISE* J121752.08+300700.6, potential counterpart associated with BZB J1217+3007, classified as a BL Lac on the basis of its featureless continuum. Lower panel: as in Figure 4.

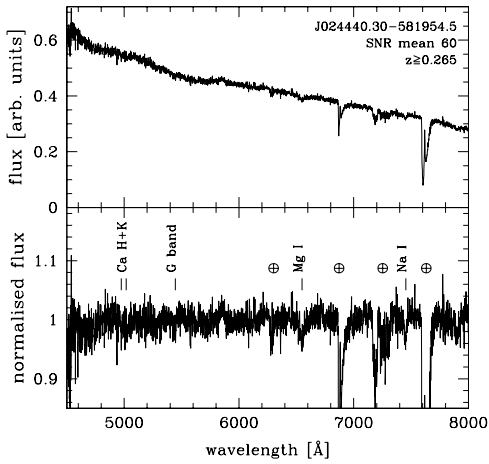


Fig. 23.— Upper panel: optical spectra observed at Magellan of *WISE* J024440.30-581954.5, potential counterpart associated with BZB J0244-5819, classified as a BL Lac since its absorption lines have $EW \lesssim 5 \text{ \AA}$. The detection of absorption lines (Ca H+K, G band, Mg I and Na I) has enabled us to estimate a lower limit on its redshift of 0.265. Lower panel: as in Figure 4.

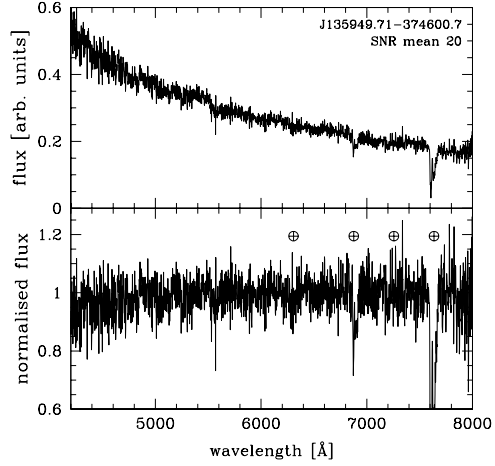


Fig. 25.— Upper panel: optical spectra observed at SOAR of *WISE* J135949.71-374600.7, potential counterpart associated with BZB J1359-3746, classified as a BL Lac on the basis of its featureless continuum. Lower panel: as in Figure 4.

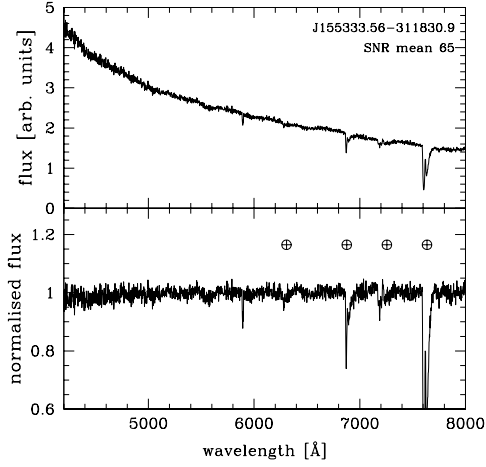


Fig. 26.— Upper panel: optical spectra observed at SOAR of *WISE* J155333.56-311830.9, potential counterpart associated with BZB J1553-3118, classified as a BL Lac on the basis of its featureless continuum. Lower panel: as in Figure 4.

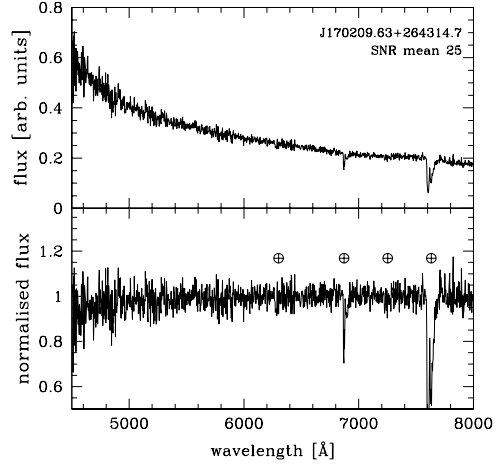


Fig. 28.— Upper panel: optical spectra observed at KPNO of *WISE* J170209.63+264314.7, potential counterpart associated with BZB J1702+2643, classified as a BL Lac on the basis of its featureless continuum. Lower panel: as in Figure 4.

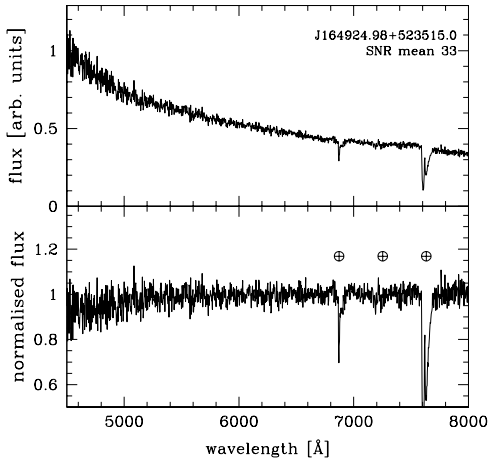


Fig. 27.— Upper panel: optical spectra observed at KPNO of *WISE* J164924.98+523515.0, potential counterpart associated with BZB J1649+5235, classified as a BL Lac on the basis of its featureless continuum. Lower panel: as in Figure 4.

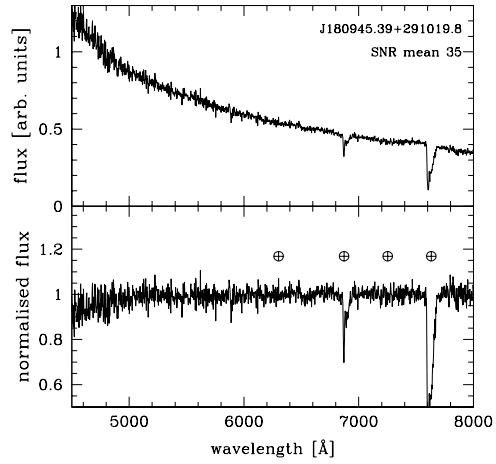


Fig. 29.— Upper panel: optical spectra observed at KPNO of *WISE* J180945.39+291019.8, potential counterpart associated with BZB J1809+2910, classified as a BL Lac on the basis of its featureless continuum. Lower panel: as in Figure 4.

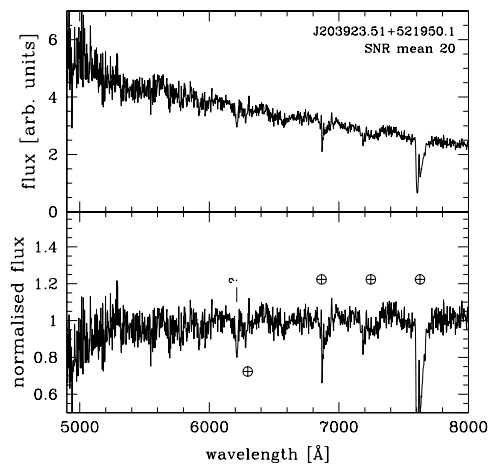


Fig. 30.— Upper panel: optical spectra observed at KPNO of *WISE* J203923.51+521950.1, potential counterpart associated with BZB J2039+5219, classified as a BL Lac on the basis of its featureless continuum. Lower panel: as in Figure 4.